

Impact of two CO₂ laser heatings for damage repairing on fused silica surface

P. Cormont,^{1,*} L. Gallais,² L. Lamaignère,¹ J. L. Rullier,¹ P. Combis,³ D. Hebert¹

¹CEA CESTA, F-33114 LE BARP, France

²Institut Fresnel, CNRS, Aix-Marseille Université, Ecole Centrale Marseille, 13013 Marseille, France

³CEA DAM Ile-de-France, F-91297 ARPAJON, France

*philippe.cormont@cea.fr

Abstract: CO₂ laser is an interesting tool to repair defects on silica optics. We studied UV nanosecond laser-induced damage in fused silica after CO₂ laser heating. The localization of damage sites and the laser damage threshold are closely related to stress area in silica induced by heating. By applying a suitable second laser heating, we managed to eliminate the debris issued from redeposited silica and to modify the stress area. As a consequence, a significant increase of laser resistance has been observed. This process offers the possibility to improve damage repairing sufficiently to extend the lifetime of the silica components.

©2010 Optical Society of America

OCIS codes: (140.3330) Lasers and laser optics: laser damage; (220.4610) Optical design and fabrication: optical fabrication; (160.6030) Materials: silica

References and links

1. P. A. Temple, W. H. Lowdermilk, and D. Milam, "Carbon dioxide laser polishing of fused silica surfaces for increased laser-damage resistance at 1064 nm," *Appl. Opt.* **21**(18), 3249–3255 (1982).
2. J. Jiao, and X. Wang, "Cutting glass substrates with dual-laser beams," *Opt. Laser Eng.*, **860** (2008).
3. R. M. Brusasco, B. M. Penetrante, J. A. Butler, S. M. Maricle, and J. E. Peterson, "CO₂ laser polishing for reduction of 351 nm surface damage initiation in fused silica," *Proc. SPIE* **4679**, 34 (2002).
4. K. M. Nowak, H. J. Baker, and D. R. Hall, "Efficient laser polishing of silica micro-optic components," *Appl. Opt.* **45**(1), 162–171 (2006).
5. E. Mendez, K. M. Nowak, H. J. Baker, F. J. Villarreal, and D. R. Hall, "Localized CO₂ laser damage repair of fused silica optics," *Appl. Opt.* **45**(21), 5358–5367 (2006).
6. R. M. Brusasco, B. M. Penetrante, J. A. Butler, and L. W. Hrubesh, "Localized CO₂ laser treatment for mitigation of 351 nm damage growth on fused silica," *Proc. SPIE* **4679**, 40–47 (2002).
7. M. A. Stevens-Kalceff, and J. Wong, "Distribution of defects induced in fused silica by ultraviolet laser pulses before and after treatment with a CO₂ laser," *J. Appl. Phys.* **97**(11), 113519 (2005).
8. S. Palmier, L. Gallais, M. Commandré, P. Cormont, R. Courchinoux, L. Lamaignère, J.-L. Rullier, and P. Legros, "Optimization of a laser mitigation process in damaged fused silica," *Appl. Surf. Sci.* **255**(10), 5532–5536 (2009).
9. S. T. Yang, M. J. Matthews, S. Elhadj, D. Cooke, G. M. Guss, V. G. Draggoo, and P. J. Wegner, "Comparing the use of mid-infrared versus far-infrared lasers for mitigating damage growth on fused silica," *Appl. Opt.* **49**(14), 2606 (2010).
10. I. L. Bass, G. M. Guss, and R. P. Hackel, "Mitigation of Laser Damage Growth in Fused Silica with a Galvanometer Scanned CO₂ Laser," *Proc. SPIE* **5991**, 59910C (2005).
11. T. A. Laurence, J. D. Bude, N. Shen, T. Feldman, P. E. Miller, W. A. Steele, and T. Suratwala, "Metallic-like photoluminescence and absorption in fused silica surface flaws," *Appl. Phys. Lett.* **94**(15), 151114 (2009).
12. M. D. Feit, and A. M. Rubenchik, "Mechanisms of CO₂ laser mitigation of laser damage growth in fused silica," *Proc. SPIE* **4932**, 91–102 (2003).
13. M. D. Feit, A. M. Rubenchik, C. D. Boley, and M. Rotter, "Development of a Process Model for CO₂ Laser Mitigation of Damage Growth in Fused Silica," *Proc. SPIE* **5273**, 145–154 (2004).
14. L. Gallais, P. Cormont, and J.-L. Rullier, "Investigation of stress induced by CO₂ laser processing of fused silica optics for laser damage growth mitigation," *Opt. Express* **17**(26), 23488–23501 (2009).
15. I. L. Bass, V. G. Draggoo, G. M. Guss, R. P. Hackel, and M. A. Norton, "Mitigation of Laser Damage Growth in Fused Silica NIF Optics with a Galvanometer Scanned CO₂ Laser," *Proc. SPIE* **6261**, 62612A (2006).
16. L. Lamaignère, M. Balas, R. Courchinoux, T. Donval, J. C. Poncetta, S. Reyné, B. Bertussi, and H. Bercegol, "Parametric study of laser-induced surface damage density measurements: Toward reproducibility," *J. Appl. Phys.* **107**(2), 023105 (2010).
17. B. Bertussi, P. Cormont, S. Palmier, P. Legros, and J.-L. Rullier, "Initiation of laser-induced damage sites in fused silica optical components," *Opt. Express* **17**(14), 11469–11479 (2009).

18. M. A. Norton, J. J. Adams, C. W. Carr, E. E. Donohue, M. D. Feit, R. P. Hackel, W. G. Hollingsworth, J. A. Jarboe, M. J. Matthews, A. M. Rubenchik, and M. L. Spaeth, "Growth of laser damage in fused silica: diameter to depth ratio," Proc. SPIE **6720**, 67200H (2007).
19. M. J. Matthews, I. L. Bass, G. M. Guss, C. C. Widmayer, and F. L. Ravizza, "Downstream Intensification Effects Associated with CO₂ Laser Mitigation of Fused Silica," Proc. SPIE **6720**, 67200A (2007).
20. S. Mainguy, B. Le Garrec, and M. Josse, "Downstream impact of flaws on the LIL/LMJ laser lines," Proc. SPIE **5991**, 599105 (2005).
21. H. Bercegol, P. Grua, D. Hébert, and J. P. Morreeuw, "Progress in the understanding of fracture related laser damage of fused silica," Proc. SPIE **6720**, 672003 (2007).
22. J. Zarzyski, "Les verres et l'état vitreux," Masson (1982).
23. See <http://hpfs@corning.com/> for #7980 product specification.
24. L. W. Hrubesh, M. A. Norton, W. A. Molander, E. E. Donohue, S. M. Maricle, B. M. Penetrante, R. M. Brusasco, W. Grundler, J. A. Butler, J. W. Carr, R. M. Hill, L. J. Summers, M. D. Feit, A. Rubenchik, M. H. Key, P. J. Wegner, A. K. Burnham, L. A. Hackel, and M. R. Kozlowski, "Methods for mitigating surface damage growth on NIF final optics," Proc. SPIE **4679**, 23 (2002).

1. Introduction

Fused silica is a widely used material for the manufacture of optical components. The glassmakers are able to produce large quantities of silica without any defect in the material. But the machining of this material creates surface fractures more or less numerous and deeply depending on the techniques of finishing the optical parts. The CO₂ lasers have been employed for a long time, as a surface post-treatment, to manufacture optical components without surface defects, thanks to superficial melting of the silica [1]. Since these early interests, several studies described how to use the CO₂ laser to improve glass cutting [2], optical polishing [3], micro-optics fabrication [4], damage repairing [5] and mitigation of damage growth [6]. In this context, strong efforts are made to extend the lifetime of large optical components used in high power laser applications [7–9]. The intense heat needed to remove damage by combination of evaporation and melting of silica, also has negative effects that generate debris [10,11] and stress [12–14] in the zone surrounding the crater formed by the laser. Silica weakening and apparition of damage around the mitigated site are major interests for the optimization of the process. To eliminate the detrimental consequences of debris a "passivation" method has been proposed using a technique based on fast galvanometer scanning [15]. Still new damage sites appeared outside the crater even in the absence of debris. Such observation can be interpreted by residual stresses producing micro-cracks which act as centres for subsequent damage formation [12]. We propose here, to study the possibility of using CO₂ laser treatment on mitigated laser damage sites of fused silica components, to render them functioning during subsequent use. We show in this paper that a second heating process with appropriate parameters permit us, not only to eliminate debris but also to significantly reduce the detrimental effect of residual stresses. Then, these results are discussed after comparison with calculated values of stresses.

2. Heating process

We used the CO₂ laser in two different ways in order to take advantage of properties of silica: a first heating to obtain silica mass ejection, and a second heating to soften the silica without mass ejection. Details of the heating laser and the movable lens used to adjust quickly and accurately the CO₂ laser beam size have been reported elsewhere [14]. For the study described here, a focal length of 20 inches enables us to obtain a beam of diameter as large as 1.6 mm on the surface to be treated. Samples, with diameter and thickness of 50 mm and 5 mm respectively, are Corning 7980 fused silica polished by SESO. Primarily, damage sites were initiated with a Nd:YAG laser delivering a pulse length of 2.5 ns at 355 nm and a diameter of 0.9 mm at 1/e² [16]. One shot was applied on several sites at fluence greater than 20 J/cm² in order to create damage sites of few tens of micrometers in radius. Then, all damage sites underwent a first CO₂ laser heating during 1 s with a beam size of 0.7 mm at 1/e² and a power of 5.5 W, to eliminate fractured silica. A second laser heating was applied on the same site during 1 s with a beam size of 1.4 mm, to transform again the silica surface but without mass ejection. We found that this is achieved if the laser power is lower than 13 W, with our experimental configuration. Figure 1 shows the impact of two successive heatings (H1 and

H2) on a surface damage (D). Surface modifications were characterized by oblique illumination microscopy (OI), followed by confocal microscopy (C) to measure the crack's depth [17].

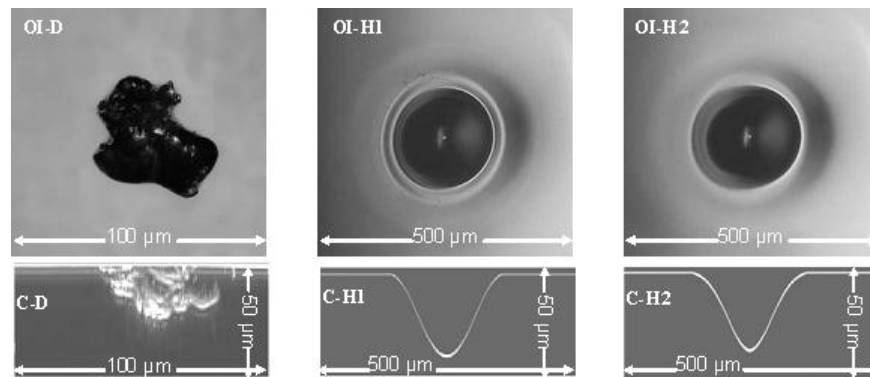


Fig. 1. The first row of images was obtained with oblique illumination microscopy (OI) and the second with confocal microscopy (C). The first column (D) is the characterization of a typical damage, the second (H1) is its transformation after the first heating by CO₂ laser, and the third (H2) shows the impact of the second heating with a power of 12.5 W on the previous crater.

As displayed by observations with microscopes, a typical damage site created by UV laser has a diameter of 60 μm and a depth of 20 μm (OI-D and C-D). This kind of damage site with a depth of several microns and numerous fractures around is critical for the optic lifetime [18]. After the first heating with the chosen parameters, the crater dimensions, diameter of 180 μm and depth of 40 μm (OI-H1 and C-H1), indicate that all fractures were removed. The second heating has apparently a negligible effect on the crater formed by the previous heating (OI-H2 and C-H2). More details of the second heating consequences are given on Fig. 2, where Nomarski microscopy (N) and dark field microscopy (DF) are shown together with interferential microscopy (I).

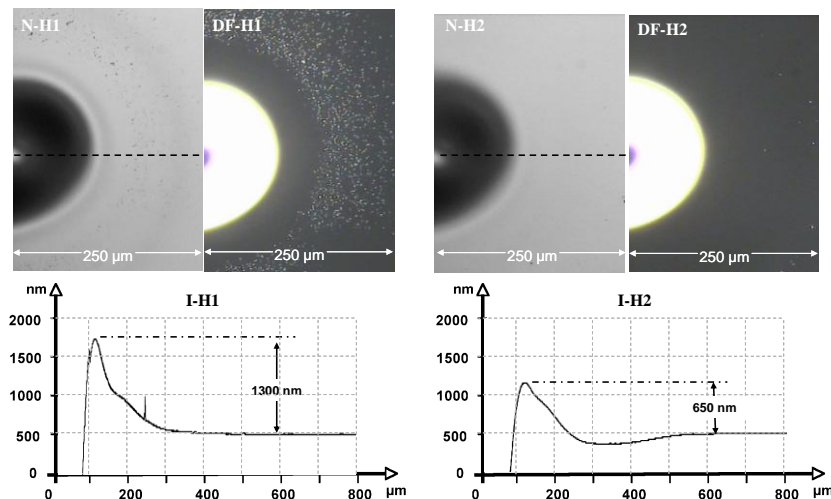


Fig. 2. The left part of the figure (H1) is the characterization of the crater formed after the first heating by CO₂ laser, and the right part (H2) shows the impact of the second heating with a power of 12.5 W on the previous crater. Images were obtained with Nomarski microscopy (N) and dark field microscopy (DF), and profiles along the dashed lines by interferential microscopy (I).

Although Fig. 1 has shown that after the first heating, surface damage sites have been successfully repaired by completely ablating away the damaged silica (C-H1), the significant

amount of ablated material which was re-deposited onto the optic surface (N-H1 and DF-H1) could lead to subsequent damage initiation [10]. However, both Nomarski microscopy and dark field microscopy show unambiguously the absence of defects after the second heating (N-H2 and DF-H2). This heating was sufficient to eliminate defects and it did not create new debris because material was not ejected. It has been shown also, that the rim created on the edge of the ablation crater can introduce intensification of transmitted UV light that may damage optics located downstream [18–20]. We could expect a reduction of this effect with the re-heating used to eliminate the defects. From profiles measured by interferential microscopy (I-H1 and I-H2), we see that without optimizing the CO₂ laser parameters in that way, the second heating smoothes already the rim on the crater by a factor two.

To complete our characterizations of the fused silica transformation induced by two successive heating onto a surface damage, we underwent polariscope measurement [14]. The Fig. 3 shows an example of polariscope (P) analysis after the three different steps previously described.

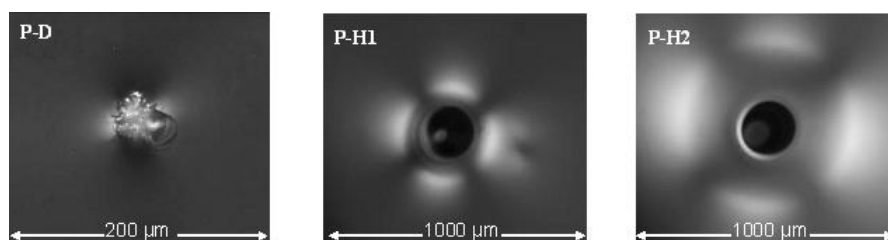


Fig. 3. Images were obtained with polariscope (P). The left image (D) is a characterization of a typical damage, the middle (H1) is its transformation after the first heating by CO₂ laser, and the right (H2) shows the impact of the second heating with a power of 12.5 W on the previous crater.

In polariscope observations, the shape of the crown is a characteristic template of the technique used and the intensity level is not directly correlated to a quantitative value of stress or constraints [14]. Moreover the signal does not indicate directly the individual stress components and also the maximum is not necessary at the surface. However, as the relative retardation in phase measured here is caused by the integrated principal stress difference along the observed beam path, it indicates an area where stress is important. In our concern, residual stress area is initially correlated with the damage including all surrounding fractures (P-D). After the first irradiation by CO₂ laser, which eliminated completely the damage, it forms a ring adjacent to the crater (P-H1). The second heating reduces these stresses sufficiently to make them invisible to the polariscope but it creates a new stress area at a greater distance from the crater (P-H2). This new zone is larger than the previous one with equivalent intensity of relative retardation. Although the second heating by CO₂ laser removes debris and smoothes crater edges, the polariscope measurement shows that it also causes the initially damaged area to spread out over a much larger surface. We now demonstrate that such a modification has a beneficial effect regarding UV laser irradiation.

3. Laser damage tests

After observations shown in previous paragraph, laser damage tests were performed, with the same Nd:YAG laser used for damage initiation, on several sites previously heated by CO₂ laser. Let us note that the beam diameter including more than 80% of the maximum fluence (300 μm) is smaller than the surface modified by the CO₂ laser. Thus, the component is translated to solicit a chosen area. The spatial profile is recorded for each shot to determine the exact peak fluence and the exact beam position. Accurate determination of the local energy distribution on the sites is then obtained. The experimental procedure consists in testing each heated site on different portion, with a single irradiation for each of them, until damage is detected. All new damage sites are visualized and localized in situ using a long working distance microscope. Figure 4 provides two examples of images obtained by the

polariscope (P) on sites heated once (H1) and twice (H1 + H2) by CO₂ laser and then tested at 355 nm.

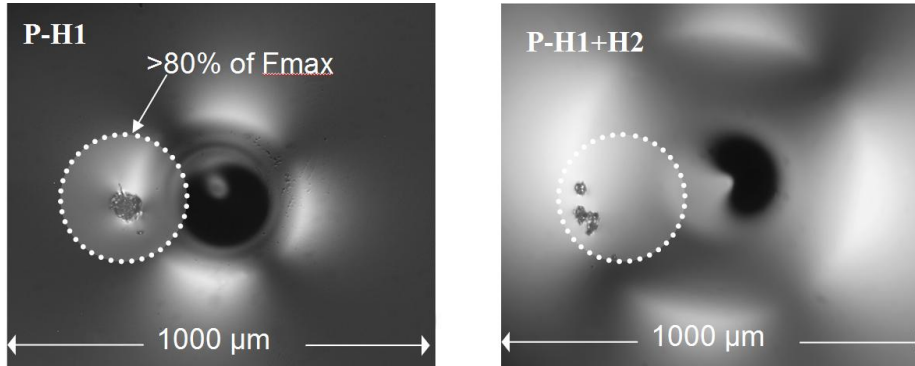


Fig. 4. Polariscope images of a site heated once by CO₂ laser then irradiated at 12 J/cm² with the Nd: YAG laser (P-H1), and of a second site heated twice by CO₂ then irradiated at 15 J/cm² with the Nd: YAG (P-H1 + H2). Area where fluence is greater than 80% of its maximum is identified by a disc.

From the left polariscope image, corresponding to a single heating by CO₂ laser (P-H1), we see that the damage created with a fluence of 12 J/cm², is located in the region of major stress. Residual debris from this heating, numerous at the bright area, could be also responsible for damage initiation. As shown previously, after the second heating by CO₂ laser, debris was eliminated and the elevated stress removed from the crater (P-H1 + H2). Accordingly, the right polariscope image shows that, even at 15 J/cm², no damage appears in this area corresponding to the central zone of the Nd:YAG laser irradiation. Nevertheless, in that case, damage sites are produced at a fluence of about 13 J/cm² in the vicinity of the new zone of observed stress, moreover in the absence of debris. This results indicates clearly the much more important contribution played by residual stresses compared with debris ejected during crater formation.

Irradiations, in which the Nd: YAG laser beam was directed to areas of high relative retardation previously measured by the polariscope, were repeated on series of 20 identical sites to evaluate a laser damage probability. With this experimental procedure, sites where damage was repaired by one heating at power of 5.5 W during 1 s with a beam diameter of 0.7 mm at 1/e², are compared with sites where damage was repaired and then heated a second time with a larger beam. For this last point, powers of 9.5 W, 11.0 W or 12.5 W were used during 1 s with a beam diameter of 1.4 mm at 1/e². Figure 5 compares the probability of damage for the different cases.

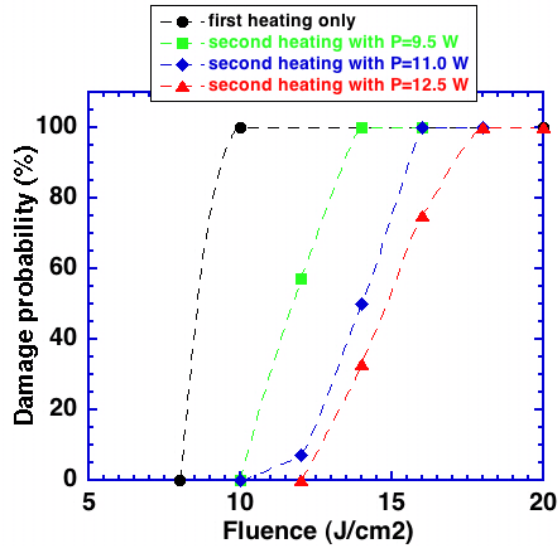


Fig. 5. Laser damage probability as a function of the fluence of irradiation at 355 nm. Before the damage test, each site had been heated by a first CO₂ laser (1 s, 0.6 mm at 1/e² and 5.5 W), then different power levels were used for the second heating (1 s and 1.4 mm at 1/e²). Each color corresponds to a value of power used for the second heating.

It has been observed [21] that fractures lead to damage at fluence as low as 5 J/cm². With our parameter of mitigation, each previously damage site undergoes fluence of 8 J/cm², but new damage sites were initiated with a fluence of 10 J/cm², for all of them. As expected, these fluences increase significantly when operating a second heating before laser damage test. The most important consequence is that a fluence greater than 12 J/cm² is needed to initiate damage if the second heating is realized at a power of 12.5 W. This work makes obvious the contribution of a second heating below the mass ejection to increase the UV laser resistance.

4. Analysis

Since the choice of the CO₂ laser parameters used for the second heating is essential for increasing the laser damage threshold, we investigate its differences with the single heating used to repair the initial damage. Primarily, we notify that a CO₂ laser irradiation realized directly on a free damage site, or as a second heating on a mitigated damage site, will have an equivalent consequence concerning the apparition of residual stress. As an illustration, we compare in Fig. 6 the case of a single irradiation on a blank site (H2) with the CO₂ laser tuned alike as the precedent “best condition” of re-heating (1 s, 1.4 mm at 1/e² and 12.5 W), and the case of two successive irradiations on a damaged site (H1 + H2) with the previous mitigating parameter (1 s, 0.6 mm at 1/e² and 5.5 W) and again the “best” second heating. Both sites were irradiated at 12 J/cm² with the Nd: YAG laser before making polariscope images (P).

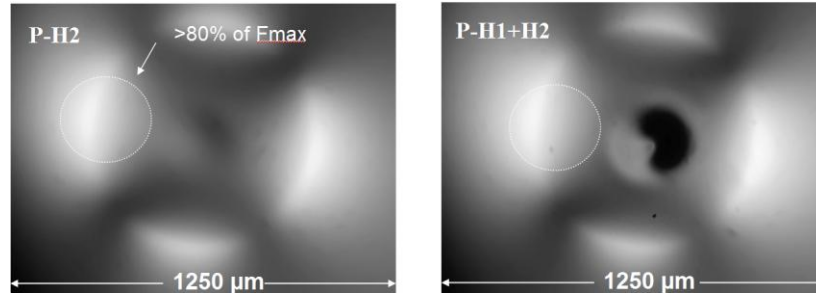


Fig. 6. Comparison between one (P-H2) and two (P-H1 + H2) CO₂ laser irradiations. Polariscope images of each site were realized after being heated by CO₂ laser and also after being UV damage tested at 12 J/cm². Area where fluence is greater than 80% of its maximum is identified by a disc.

From these images it comes out a strong similarity between a site of free silica heated once (P-H2) and one previously mitigated (P-H1 + H2), in what concerns the bright outer rings encircling the central craters. Moreover, for both situations no damage appeared at a fluence of 12 J/cm², in good accordance with the laser damage probability evaluated earlier. Consequently, we will consider the case of a “second heating” alone (P-H2), without prior mitigation for comparison with the case of a single heating used to repair the initial damage (P-H1). Thanks to a 2D axi-symmetric numerical model developed elsewhere including the data on fused silica given by glass manufacturers [14], we have calculated the temperatures (T) reached as the CO₂ laser shut-off. Results of our simulations are given in Fig. 7, where arrows point out the CO₂ laser diameter at 1/e², and the white line indicates the crater whose dimensions are known from prior experimental measurement for the mitigation case (H1) *ie* diameter of 180 μm and depth of 40 μm.

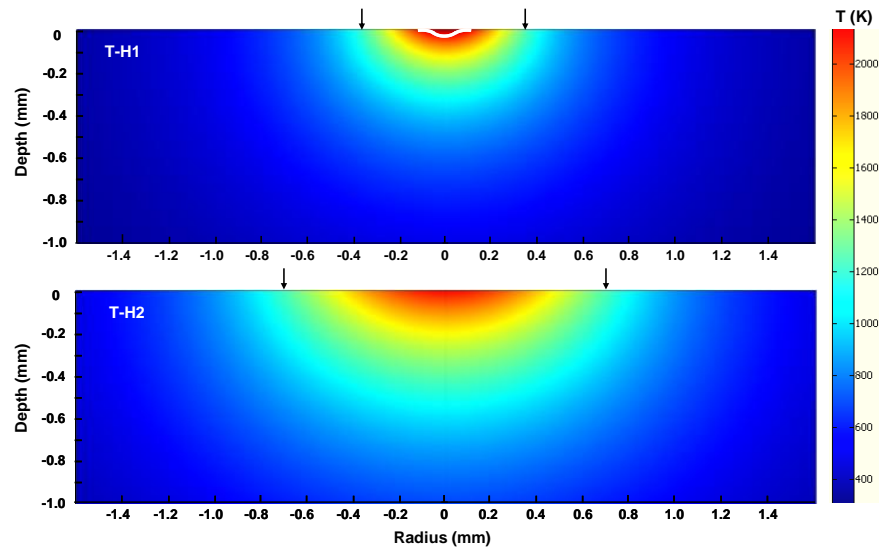


Fig. 7. Calculated temperature distribution in fused silica at the end of the CO₂ laser irradiations for parameters of one repairing irradiation (T-H1) and one re-heating irradiation (T-H2). For mitigation (T-H1), the white line delimits the crater.

The border of the crater follows an isotherm of the spatial distribution, and a temperature not much superior than 2000°K seems necessary to shape it. As the calculated temperature in the crater vicinity is not valid because the material ejection during the crater formation is not included in the model, our simulation keeps going correct as long as the temperature stay lower than about 1850°K ± 50°K. From these simulations, it can be seen that the heated area

extends far beyond from the location of the maximum temperature and decrease slowly with distance. While parameters for repairing or re-heating are significantly different, comparable temperature is reached at the edge of the CO₂ laser beam as indicated by arrows. That result shows evidence of the important role of the heating beam size, and its consequence concerning UV laser resistance.

After the fast laser turn-off, when the material cools down, the viscosity of silica rapidly increases [22] and stresses cannot be relieved by materials displacements. As observed previously, the region of these main residual stresses shaped a donut where damage created after UV irradiation is located. For the single heating used to repair the initial damage (P-H1) this area includes diameter varying between 320 and 480 μm, and for the case of a “second heating” alone (P-H2) from 600 to 900 μm. By comparing these ranges with Fig. 7, it appears that whatever the irradiation parameters this area corresponds to a calculated temperature reached at the end of the pulse between 1650 and 1900°K.

For the silica of our study the transition from 'soft' to solid material is reached at 1858°K [23], and for temperature lower than this softening point, because of the very high viscosity (10^{7.6} poisses), stresses can be considered as imprinted into the material after heating ([12]). Then we consider that below a temperature of 1850°K the residual stress present in the material relates to the stress at the end of the pulse. The authors have pointed out the possibility of cracks production during the initiation process. Confrontations between our experiment and simulation are given in Fig. 8, where the observed zone of new damage (after testing with the Nd:YAG laser) is positioned on the calculated stress repartition. Each image corresponds to one of the case (H1) and (H2) under study for both radial (RS) and hoop (HS) stress.

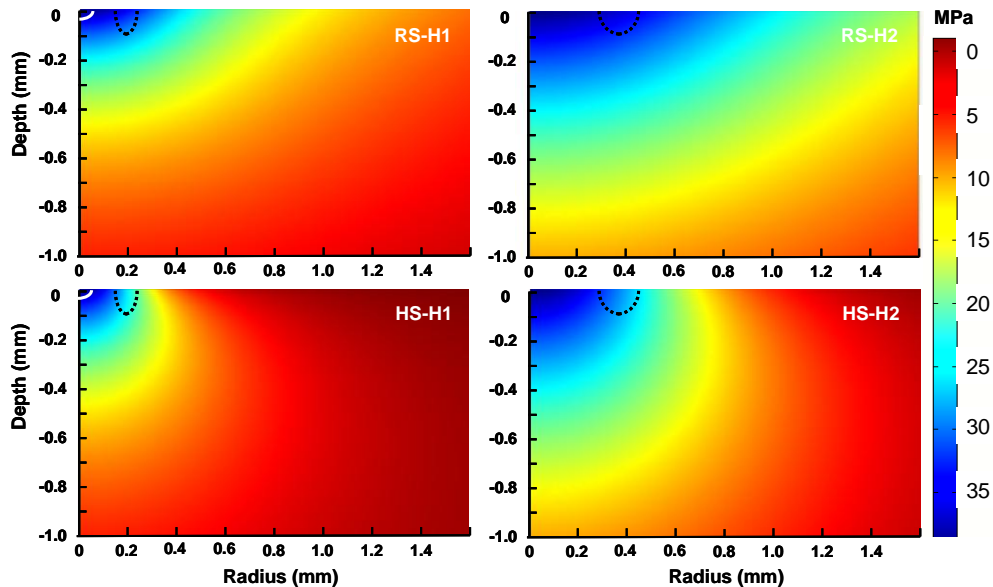


Fig. 8. Calculated stress repartition in fused silica at the end of the CO₂ laser irradiations for parameters of one repairing irradiation (H1) and one re-heating irradiation (H2). Radial stresses are represented in the upper part (RS), and hoop at the lower (HS). For mitigation (H1), the white line delimits the crater and zones of potential damage with dashed lines.

Similar behavior is obtained for both cases, and the stress area expands following the heating beam size. The radial stress (RS) decreases with distance from the crater, and the contours of constant stress maintain a shape similar to the crater even if this later is not formed. The hoop stress (HS) also exhibits this behavior, but decreases much more rapidly along the silica-air interface. The shear stress was also calculated but was found to have a maximum of only 0.5 MPa in both case H1 and H2, which is about two orders of magnitude

lower than radial and hoop stresses. The more important outcome from these calculations is that at the localization of the potential new damage encircled by a black dashed line, an equivalent level of stress is reached, while the probability of damaging has been measured drastically different, *ie* 100% of new damage at 10 J/cm² for (H1) and 18 J/cm² for (H2). The rapid decrease of the hoop stress along the silica-air interface produces a gradient of stress clearly different in both cases. This effect could explain such damage resistance disparity, and then correlates its increase with the use of a larger size of beam.

5. Conclusion

The CO₂ laser is one of the best tools to mitigate the damage growth in fused silica components of a laser power chain [24]. Fractures around damaged site are completely eliminated by heating the silica with suitable CO₂ laser parameters. However, this operation that requires ejection of matter is nearby painful, and maintaining the required good qualities of silica component is one of the major challenges for large facilities. To achieve this objective, we have proposed to run a second time the CO₂ laser on the mitigated site, but with different beam parameters. During this second heating, the temperature remains in the range between the annealing point and the softening point of silica. With an experimental study we have evaluated the laser damage probability as a function of the CO₂ laser parameters. The surface evolution followed by polariscope leads us to believe that the constraints are an important contributor to the weakness in laser induced damage. But complementary analyses are needed to understand more precisely the peculiar role of the different stresses. Finally, we have demonstrated that the use of a second heating allows a reorganization of the material where its damage threshold, is significantly increased.